

## Mechanical properties and fracture mechanisms of aluminum matrix composites reinforced by $Al_9(Co, Ni)_2$ intermetallics

CHENG Su-ling(程素玲), YANG Gen-cang(杨根仓), ZHU Man(朱满),  
WANG Jin-cheng(王锦程), ZHOU Yao-he(周尧和)

State Key Laboratory of Solidification Processing, Northwestern Polytechnical University, Xi'an 710072, China

Received 2 March 2009; accepted 26 May 2009

**Abstract:** The microstructures and mechanical properties of Al matrix composites reinforced by different volume fractions of Al-Ni-Co intermetallic particles were investigated. Three different volume fractions of Al-Ni-Co particles were added to pure Al matrix using a stir-casting method. Microstructural analysis shows that with the increasing of the reinforcement volume fraction, the matrix grain size decreases and the porosity increases. The mechanical properties of the composites are improved over the matrix materials, except for the decreasing of the ductility. Fracture surface examination indicates that there is a good interfacial bonding between the Al matrix and the Al-Ni-Co particles and the fracture initiation does not occur at the particle-matrix interface.

**Key words:** aluminium matrix composites; Al-Ni-Co quasicrystal; mechanical properties; intermetallics

### 1 Introduction

Aluminium matrix composites (AMCs) reinforced with ceramic particles have been much developed as structural components in the automotive and aerospace industries because of their excellent properties such as high specific stiffness, high strength and high abrasion resistance[1–3]. An inherent difficulty in the fabrication of the AMCs is the poor wettability between the ceramic particles and the Al matrix. It is well known that intermetallics (IMs) can be wetted by molten metal easily. Moreover, they exhibit comparable mechanical properties and closer coefficient of thermal expansion (CTE) with Al when compared to ceramic materials[4]. Therefore, IMs based on Ni-Al (mainly  $Ni_3Al$  and NiAl) and Ti-Al (mainly TiAl) systems have recently been studied as a new family of reinforcements of AMCs [5–7]. The stiffness and wear behavior of the AMCs can be improved by the intermetallics addition.

Quasicrystals (QCs) as a kind of IMs are found to exhibit high hardness and strength [8–9]. An Al-Cu-Fe QC was suggested to be used as particle reinforcement for AMCs fabricated by mechanical alloying (MA)

method by TSAI et al for the first time[10]. Then QI et al[11–12] studied the phase transformation and wear properties of the AMCs reinforced with Al-Cu-Cr quasicrystalline particles produced by powder metallurgical (PM) technique. More recently, TANG et al [13] and CHERDYNTSEV et al[14–15] fabricated Al-Cu-Fe quasicrystalline particles reinforced AMCs by PM technique. It was found that as the consolidation temperature exceeds about 500 °C, atomic diffusion between the Al matrix and the quasicrystalline particles takes place, and the quasicrystalline phase transforms to a crystalline phase, which has a higher Al content as compared to that in the quasicrystalline phase[13, 15]. Mechanical property tests reveal that the phase transformation is accompanied by the hardness decrease and strength increase of the AMCs[14–15].

Besides MA and PM methods used in the fabrication of the AMCs reinforced with quasicrystalline particles mentioned above, casting method was also selected by LEE et al to fabricate AMCs reinforced with Al-Cu-Fe QC-containing particles[16]. They found that the volume fraction of the quasicrystalline phase in the Al-Cu-Fe particles decreases and that of the co-existing crystalline phase increases during the casting process,

accompanied by the dissolution of the smaller particles into the Al matrix. In contrast, as reported in Ref.[17],  $\text{Al}_{72}\text{Ni}_{12}\text{Co}_{16}$  single QC was used as particulate reinforcement added to pure Al matrix by a stir-casting method. Microstructural analysis of the composite indicates that the quasicrystalline phase transforms completely to the crystalline phase  $\text{Al}_9(\text{Co}, \text{Ni})_2$  during the fabrication process. In addition, the particle size of the resulting  $\text{Al}_9(\text{Co}, \text{Ni})_2$  IMs particles was remarkably smaller than that of the original Al-Ni-Co quasicrystalline particles due to particle fragmentation [17]. Tensile tests indicate that the ultimate tensile strength (UTS), yield strength (YS) and elastic modulus (EM) of the as-cast composite were improved over the matrix properties remarkably.

However, in Ref. [17], only one volume fraction of the Al-Ni-Co quasicrystalline particles was added to the Al matrix. To investigate the effect of the particle volume fraction on the microstructures and mechanical properties of the Al matrix, in this work, various volume fractions of the Al-Ni-Co quasicrystalline particles were added to the Al matrix. Also, the failure mechanism of the composites was discussed by fracture surface analyses.

## 2 Experimental

The  $\text{Al}_{72}\text{Ni}_{12}\text{Co}_{16}$  quasicrystalline particles were fabricated by conventional casting method. The microstructure analysis showed that the ingot has a single-QC structure. The preparation and characterization of the  $\text{Al}_{72}\text{Ni}_{12}\text{Co}_{16}$  quasicrystalline particles were introduced detailedly in Ref.[17]. The particles within a size range of 100–150  $\mu\text{m}$  were selected for synthesizing composites.

Three particle volume fractions, 7%, 10% and 15%, were introduced to a commercial Al (99.8%) matrix by the stir-casting method as introduced in Ref.[17]. The three composites were designated as C7, C10 and C15 hereinafter. The composites C7 and C10 were cast at 700  $^{\circ}\text{C}$ , while C15 was cast at 710  $^{\circ}\text{C}$  to guarantee adequate fluidity. The microstructures of the composites were analyzed by scanning electron microscopy (SEM).

Densities were measured by water displacement technique. The measured densities were compared to the values obtained using the rule of mixtures (ROM) so as to determine the volume fractions of porosity of the composites [18].

Tensile tests were performed at a strain rate of 0.3 mm/min on round specimens with a diameter of 5 mm and gauge length of 25 mm at room temperature. Fracture surfaces of the tested samples were examined by SEM.

## 3 Results and discussion

### 3.1 Microstructures

The typical microstructures of the as-cast composites with different volume fractions of the Al-Ni-Co particles are shown in Fig.1. In all the samples, polygonal morphology particles and Al matrix with an

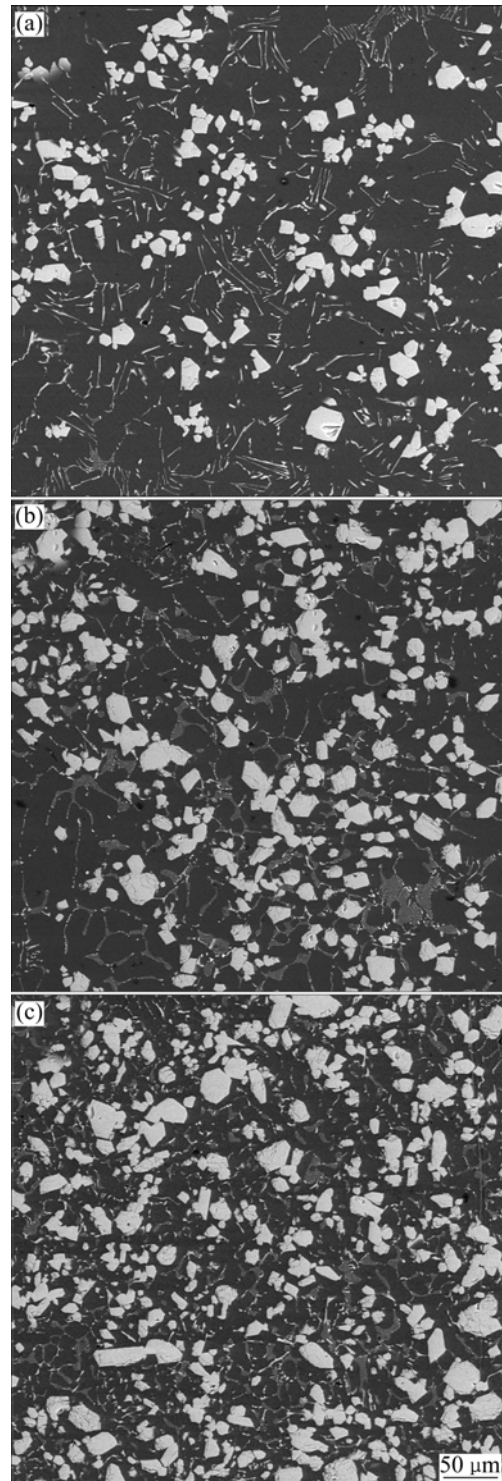


**Fig.1** Backscattered electron (BSE) images of composite: (a) Sample C7; (b) Sample C10; (c) Sample C15

eutectic structure formed in the interdendritic region can be seen. The polygonal phase and eutectic structure have been identified to be  $\text{Al}_9(\text{Co}, \text{Ni})_2$  phase and Al,  $\text{Al}_3(\text{Ni}, \text{Co})$  and  $\text{Al}_9(\text{Co}, \text{Ni})_2$  ternary eutectic, respectively, according to the Al-Ni-Co ternary phase diagram combined with X-ray diffraction (XRD) and energy dispersive spectroscopy (EDS) analysis[17]. The particles are mostly embedded in the Al grains while others are along the grain boundaries with eutectic phases. The particle distribution is relatively uniform, though particle-rich and particle-free regions can be seen due to the effect of solidification. The particle size of the  $\text{Al}_9(\text{Co}, \text{Ni})_2$  phase in the three composites is mostly in a range of 15–25  $\mu\text{m}$ , which is much smaller than that of the starting quasicrystalline particles (100–150  $\mu\text{m}$ ). The reason of the particle size decreasing is particle fragmentation as preliminary discussed in Ref.[17] and will be studied detailedly in a subsequent article. On the other hand, the matrix grain size dramatically decreases with increasing volume fraction of the reinforcement particles (Fig.1).

The matrix grain size decreases with increasing amount of the reinforcement particles is confirmed by the grain size measurement conducted by line-cross method (Table 1). The porosities of the studied samples are also listed in Table 1. As widely observed in particle reinforced metal matrix composites (PRMMCs), the matrix grain size decreases and the porosity increases with increasing the volume fraction of the reinforcement particles.

**Table 1** Characterization results of Al matrix and three composites

Sample	Experimental density/ ( $\text{g}\cdot\text{cm}^{-3}$ )	Theoretical density/ ( $\text{g}\cdot\text{cm}^{-3}$ )	Porosity/ %	Grain size/ $\mu\text{m}$
Al	2.67±0.01	2.70	1.11	–
C7	2.73±0.01	2.78	1.80	28
C10	2.77±0.01	2.82	1.77	22
C15	2.79±0.01	2.87	2.79	19

In general, when ceramic particles are introduced to a metal matrix by casting method, particle-porosity clusters tend to occur due to the poor wettability and gas entrapment during mixing[19–21]. However, the defect has not been found in the present study, which can be attributed to several aspects. Firstly, the good wettability of the Al-Ni-Co IM particles with Al melt helps the dispersion process of the particles in the Al melt. Secondly, the gas entrapment during the mixing is much less due to the fairly big size of the original Al-Ni-Co

quasicrystalline particles, compared to that in the case of adding finer particles with the equivalent volume fractions. Finally, as mentioned above, the particle fragmentation occurs in the Al melt, giving rise to a clean surface, which can form an intimate contact with the Al melt and obtain a perfect metallurgical bonding after solidification without impurities or gas presenting at particle-matrix interface.

### 3.2 Tensile properties and fracture surface examination

The average measured tensile properties of all the samples are given in Table 2. The 0.2% offset yield stress (YS) and ultimate tensile strength (UTS) of the composites are higher than those of the Al matrix, and show a monotonic trend over the whole added reinforcement volume fractions. The data of Al/SiC<sub>p</sub> composites from Ref.[22], in which 20SiC-cast and 20SiC-PM indicate AMCs reinforced with 20% (volume fraction) SiC with an average size of 250  $\mu\text{m}$  fabricated by casting method and powder metallurgy method, are also shown in Table 2. It can be seen that the strengthening efficiency of the Al-Ni-Co particles for pure Al matrix is superior to that of 250  $\mu\text{m}$  SiC particles in both as-cast and PM state. This may be attributed to several factors including the good particle-matrix interfacial bonding, the fine reinforcement particle size, the strengthening effect of elemental Ni and Co on the Al matrix as well as the presence of the  $\text{Al}_3(\text{Ni}, \text{Co})$  phase in the composites studied here.

**Table 2** Tensile properties of composites and pure Al matrix

Sample	YS/MPa	UTS/MPa	EF/%	EM/GPa
Al	37	64	30	68
C7	49	83	3	71
C10	52	87	2	75
C15	63	104	<1	72
20SiC-cast	47.9	71.9	–	–
20SiC-PM	56	86.9	–	–

However, the elastic modulus (EM) of the studied materials reaches a maximum value when the particle volume fraction is 10%, and decreases afterward (Table 2). The decrease of the EM of sample C15 may be attributed to the increasing of porosity (see Table 1), which can be confirmed by the fracture surface analysis of sample C15 to be discussed in a subsequent paragraph. It was found that the porosity can reduce the EM of a PRMMC[23–25]. LING et al[25] produced AMCs reinforced with up to 30% (volume fraction) SiC by PM technique and studied the mechanical property variation

with the volume fraction of SiC particles. They found that the EM increased at 10% SiC loading, kept constant at 20%, and dropped at 30%. The drop was explained by the increased porosity in the composite containing 30% SiC.

The level of the ductility of the three composites is low. The increase of reinforcement content decreases the elongation fracture (EF) of the composites. Generally, the fracture of reinforcement particle and the localization of matrix deformation are considered as the main factors to be responsible for the decrease of the ductility of PRMMCs[26–28]. With the reinforcement volume fraction increasing, the geometric slip distance of the dislocation decreases, the microcracks occur at a relatively low elongation rate, and the EF decreases consequently[27–28].

Fig.2 shows the typical fractographs of the failed tensile samples. All of the samples display a mixed fracture mechanism on the fracture surface: brittle fracture of the reinforcement particles and ductile tearing of the Al matrix. A primary difference between the fracture surfaces of the three composites is the relative area fraction of the matrix to fractured particles. With the particle volume fraction increasing, the fractured particles increase. Another difference is the proportion of voids presented on the fracture surface (see rectangles in Figs.2(b) and (c)). It can be concluded from Fig.2 that the dominant fracture mode of samples C7 and C10 is particle cracking and matrix ductile tearing, while the fracture of sample C15 is primarily initiated from shrinkage cavities. The fracture surface examination is consistent with the decrease of the EM after the reinforcement particle volume fraction reaches 15%. Particle-matrix interfacial debonding can not be found by the fracture surface examination, which confirms the strong interfacial bonding between the IM particles and the Al matrix.

#### 4 Conclusions

AMCs reinforced with different volume fractions of Al-Ni-Co particles were fabricated by stir-casting method. The microstructures and mechanical properties of the composites were characterized and conclusion can be drawn:

1) The microstructure analysis of the composites reveals the uniform distribution of the Al-Ni-Co particles. The increase in reinforcement volume fraction results in the increase of the porosity and decrease of matrix grain size in the composites.

2) The UTS and YS of the composites increase continuously with the increase of reinforcement content,

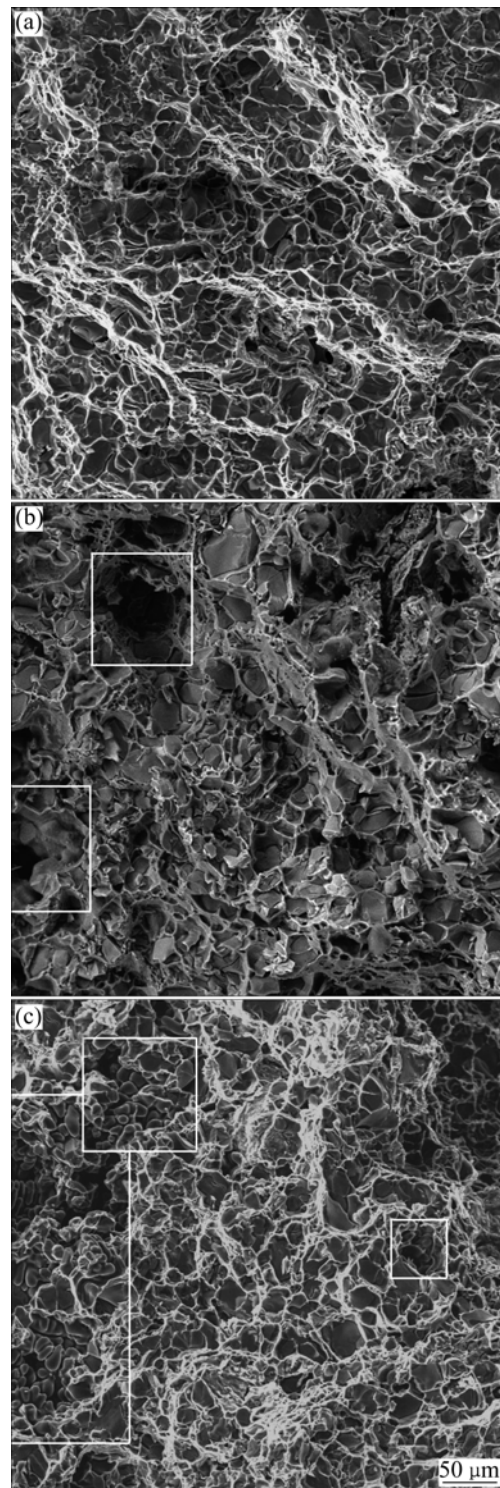


**Fig.2** SEM images showing typical fracture surfaces of failed tensile composites: (a) Sample C7; (b) Sample C10; (c) Sample C15

while the EF exhibits an inverse trend. The EM increases up to 10% Al-Ni-Co particles, and decreases at 15%.

3) The fractures of samples C7 and C10 are initiated from particle cracking, while that of sample C15 is induced by shrinkage cavities, which results in the

decreased value of the EM.

## References

- [1] HOOKER J A, DOORBAR P J. Metal matrix composites for aeroengines [J]. *Mater Sci Technol*, 2000, 16: 725–731.
- [2] KACZMAR J W, PIETRZAK K, WLOSINSKI W. The production and application of metal matrix composite materials [J]. *J Mater Process Tech*, 2000, 106: 58–67.
- [3] BREVAL E. Synthesis routes to metal matrix composites with specific properties: A review [J]. *Compos Eng*, 1995, 5: 1127–1133.
- [4] VARIN R A. Design of a low-melting point metal matrix composite reinforced with intermetallic ribbons [J]. *Z Metallkde*, 1990, 81: 373–379.
- [5] POUR H A, LIEBLICH M, LÓPEZ A J, RAMS J, SALEHI M T, SHABESTARI S G. Assessment of tensile behaviour of an Al-Mg alloy composite reinforced with NiAl and oxidized NiAl powder particles helped by nanoindentation [J]. *Composites: Part A*, 2007, 38: 2536–2540.
- [6] MUÑOZ-MORRIS M A, REXACH J I, LIEBLICH M. Comparative study of Al-TiAl composites with different intermetallic volume fractions and particle sizes [J]. *Intermetallics*, 2005, 13: 141–149.
- [7] COSTA C E D A, VELASCO F, TORRALBA J M. Mechanical, intergranular corrosion, and wear behavior of aluminum-matrix composite materials reinforced with nickel aluminides [J]. *Metall Mater Trans A*, 2002, 33: 3541–3553.
- [8] WOLF B, BAMBAUER K O, PAUFLER P. On the temperature dependence of the hardness of quasicrystals [J]. *Mater Sci Eng A*, 2001, 298: 284–295.
- [9] GIACOMETTI E, BALUC N, BONNEVILLE J, RABIER J. Microindentation of Al-Cu-Fe icosahedral quasicrystal [J]. *Scripta Mater*, 1999, 41: 989–994.
- [10] TSAI A P, AOKI K, INOUE A, MASUMOTO T. Synthesis of stable quasicrystalline particle-dispersed Al base composite alloys [J]. *J Mater Res*, 1993, 8: 5–7.
- [11] QI Y H, ZHANG Z P, HER Z K, DONG C. Phase transformation and properties of quasicrystal particles/Al matrix composites [J]. *Transactions of Nonferrous Metals Society of China*, 2000, 10: 358–363.
- [12] QI Y H, ZHANG Z P, HER Z K, DONG C. The microstructure analysis of Al-Cu-Cr phases in  $Al_{65}Cu_{20}Cr_{15}$  quasicrystalline particles/Al base composites [J]. *J Alloy Compd*, 1999, 285: 221–228.
- [13] TANG F, ANDERSON I E, BNAUPEL-HEROLD T, PRASK H. Pure Al matrix composites produced by vacuum hot pressing: tensile properties and strengthening mechanisms [J]. *Mater Sci Eng A*, 2004, 383: 362–373.
- [14] CHERDYNTSEV V V, KALOSHKIN S D, TOMILIN I A, SHELEKHOV E V, LAPTEV A I, STEPASHKIN A A. Structure and properties of mechanically alloyed composite materials Al/Al-Cu-Fe quasicrystal [J]. *Phys Met Metallogr*, 2007, 104: 497–504.
- [15] KALOSHKIN S D, TCHERDYNTSEV V V, LAPTEV A I, STEPASHKIN A A, AFONINA E A, POMADCHIK A L. Structure and mechanical properties of mechanically alloyed Al/Al-Cu-Fe composites [J]. *J Mater Sci*, 2004, 39: 5399–402.
- [16] LEE S M, JUNG J H, FLEURY E, KIM W T, KIM D H. Metal matrix composites reinforced by gas-atomised Al-Cu-Fe powders [J]. *Mater Sci Eng A*, 2000, 294/296: 99–103.
- [17] CHENG S L, YANG G C, WANG J C, YANG C L, ZHU M, ZHOU Y H. Microstructure and mechanical properties of an Al-Ni-Co intermetallics reinforced Al matrix composite [J]. *J Mater Sci*, 2010, 45: 1438–1442.
- [18] PLDDAR P, SRIVASTAVA V C, DE P K, SAHOO K L. Processing and mechanical properties of SiC reinforced cast magnesium matrix composites by stir casting process [J]. *Mater Sci Eng A*, 2007, 460/461: 357–364.
- [19] TEKMEK C, OZDEMIR I, COCEN U, ONEL K. The mechanical response of Al-Si-Mg/SiC<sub>p</sub> composite: Influence of porosity [J]. *Mater Sci Eng A*, 2003, 360: 365–371.
- [20] CÖCEN Ü, ÖNEL K. The production of Al-Si alloy-SiC<sub>p</sub> composites via compocasting: Some microstructural aspects [J]. *Mater Sci Eng A*, 1996, 221: 187–191.
- [21] SAMUEL A M, GOTMARE A, SAMUEL F H. Effect of solidification rate and metal feedability on porosity and SiC/Al<sub>2</sub>O<sub>3</sub> particle distribution in an Al-Si-Mg (359) alloy [J]. *Compos Sci Technol*, 1995, 53: 301–315.
- [22] ARSENAULT R J, WU S B. A comparison of PM vs melted SiC/Al composites [J]. *Scripta Metal*, 1988, 222: 767–772.
- [23] THAM L M, SU L, CHENG L, GUPTA M. Micromechanical modeling of processing-induced damage in Al-SiC metal matrix composites synthesized using the disintegrated melt deposition technique [J]. *Mater Res Bull*, 1999, 34: 71–79.
- [24] SLIPENYUK A, KUPRIN V, MILMAN Y, GONCHARUK V, ECKERT J. Properties of P/M processed particle reinforced metal matrix composites specified by reinforcement concentration and matrix-to-reinforcement particle size ratio [J]. *Acta Mater*, 2006, 54: 157–166.
- [25] LING C P, BUSH M B, PERERA D S. The effect of fabrication techniques on the properties of Al-SiC composites [J]. *J Mater Process Tech*, 1995, 48: 325–331.
- [26] SEGURADO J, GONZÁLEZ, LLORCA J. A numerical investigation of the effect of particle clustering on the mechanical properties of composites [J]. *Acta Mater*, 2003, 51: 2355–2369.
- [27] SONG M, HE Y H, WU Z G, HUANG B Y. Multi-scale model for the ductility of multiple phase materials [J]. *Mech Mater*, 2009, 41: 622–633.
- [28] SONG M, HUANG D W. Experimental and modeling of the coupled influences of variously sized particles on the tensile ductility of SiC<sub>p</sub>/Al metal matrix composites [J]. *Metall Mater Trans A*, 2007, 38: 2127–2137.

(Edited by FANG Jing-hua)